Chemosphere 287 (2022) 132297

Contents lists available at ScienceDirect

Chemosphere

journal homepage: www.elsevier.com/locate/chemosphere

Comparison of Zn–Al and Mg–Al layered double hydroxides for adsorption of perfluorooctanoic acid

Jingwan Huo [a], Xiaopeng Min [a], Qianqian Dong [a], Shangping Xu [b], Yin Wang [a,*]

[a] Department of Civil and Environmental Engineering, University of Wisconsin-Milwaukee, Milwaukee, WI, 53201, USA
[b] Department of Geosciences, University of Wisconsin-Milwaukee, Milwaukee, WI, 53201, USA

HIGHLIGHTS

- Cation composition of LDHs strongly affected PFOA adsorption.
- Zn–Al LDH had better performance for PFOA adsorption than Mg–Al LDH.
- Zn–Al LDH was efficient for the removal of medium- and long-chain PFCAs.
- Zn–Al LDH could be readily regenerated and reused for PFOA removal.
- Electrostatic interactions were the primary mechanism for PFOA adsorption onto LDHs.

GRAPHICAL ABSTRACT

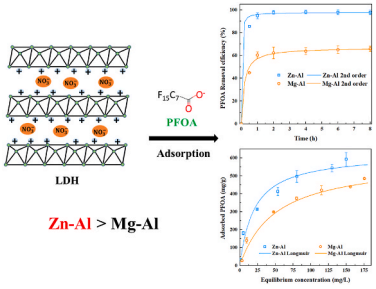

ARTICLE INFO

Handling Editor: Yongmei Li

Keywords:
Layered double hydroxide
PFAS
PFOA
Adsorption
Water treatment

ABSTRACT

Per-and polyfluoroalkyl substances (PFAS), a large class of synthesized chemicals, are persistent in nature and generally recalcitrant to conventional chemical and biological treatment. Adsorption is considered an economical and practical method for PFAS treatment. Layered double hydroxides (LDHs) represent a promising class of mineral-based adsorbents for PFAS removal because of the highly positive charge of their structural layers. In this research, the performance of two representative LDHs with varied cation compositions, namely Zn–Al and Mg–Al LDHs, were investigated and compared for the removal of perfluorinated carboxylic acids (PFCAs) with an emphasis on perfluorooctanoic acid (PFOA). Zn–Al LDH showed high efficiency for the removal of medium- and long-chain PFCAs (i.e., $C \geq 7$), and performed consistently better than Mg–Al LDH. Based on detailed adsorption kinetics and isotherm studies toward PFOA, Zn–Al LDH showed higher adsorption capacity, stronger adsorption affinity, and faster kinetics than Mg–Al LDH. Presence of natural organic matter had minimal impact on PFOA removal by Zn–Al LDH, but sulfate severely inhibited PFOA adsorption. Combined results of aqueous adsorption experiments and sorbent characterization suggested that electrostatic interactions may be the primary mechanism for PFOA adsorption onto LDHs. Our results suggested that cation composition of LDHs can have significant effect on the performance for PFCA removal.

* Corresponding author. 3200 N. Cramer St., Milwaukee, WI, 53211. USA.
E-mail address: wang292@uwm.edu (Y. Wang).

https://doi.org/10.1016/j.chemosphere.2021.132297
Received 5 July 2021; Received in revised form 30 August 2021; Accepted 17 September 2021
Available online 18 September 2021

1. Introduction

Per-and polyfluoroalkyl substances (PFAS) are a huge class of synthesized chemicals gaining increasing attention in recent years (Wang et al., 2017). Due to their unique physical and chemical properties, PFAS have been widely used in different applications in daily life, such as firefighting foams, cosmetics, food packaging products, etc. (Kotthoff et al., 2015; Ji et al., 2020). Many PFAS, including perfluoroalkyl acids (PFAAs), are very persistent in nature and generally recalcitrant to biological and chemical decomposition, because of the stable C–F bond (Merino et al., 2016; Cousins et al., 2020). Although some PFAS may partially degrade in the environment, they may ultimately transform into the highly stable end products, such as PFAAs, which are negatively charged and highly soluble in water under ambient pH conditions (Wang et al., 2013, 2015; Xiao et al., 2018). Perfluorooctanoic acid (PFOA) and perfluorooctane sulfonate (PFOS) are two legacy PFAAs that have drawn most attention in the scientific and regulation communities, and have been widely found in soil, sediment, surface water, groundwater, and tap water (Kunacheva et al., 2012; Hu et al., 2016; Wang et al., 2017; Sharifan et al., 2021). The U.S. Environmental Protection Agency (EPA) has established the lifetime drinking water health advisory levels of 70 ng/L for PFOA and PFOS, both individually and combined (EPA, 2016).

Adsorption is considered a practical and economical method to treat PFAS-contaminated water, because of its effectiveness and easy operation (Wanninayake, 2021). Various adsorbents, such as activated carbon, ion exchange resins, organic-inorganic composite materials, and advanced polymers, have been investigated for PFAS removal (Xiao et al., 2017; Ateia et al., 2019; Zhang et al., 2019; Dixit et al., 2021). Among them, activated carbon is the most widely used adsorbent to treat PFAS and its performance has been demonstrated in some field applications (Du et al., 2014; Espana et al., 2015). However, activated carbon exhibits several limitations, such as slow adsorption kinetics, unsatisfactory adsorption capacities, and reduced performance in the presence of dissolved organic carbon (Du et al., 2014; Zhang et al., 2019). For instance, it has been reported that PFOS and PFOA adsorption by granular activated carbon (GAC) required up to seven days to reach equilibrium, due to the slow intraparticle diffusion process (Yu et al., 2009). The adsorption capacities of PFOS and PFOA by activated carbon were substantially reduced in the presence of organic matters (Yu et al., 2012). Thus, it is still of great desire to develop efficient and cost-effective adsorbents for the removal of PFAS in aqueous solution.

Layered double hydroxides (LDHs) are a class of layered minerals consisting of positively charged brucite-like structural layers and exchangeable anions within the interlayers (Mishra et al., 2018). They can be typically described by the formula of $[M^{2+}_{1-x}N^{3+}_{x}(OH)_2]^{x+}(A^{n-})_{x/n}\bullet mH_2O$, where M^{2+} and N^{3+} are metal cations occupying the octahedral centers in the infinite hydroxide layers and A^{n-} is an exchangeable anion (Wang and O'Hare, 2012). LDHs are generally hydrophilic in nature, and the positively charged structural layers can provide strong electrostatic interactions to anions, thus making them suitable for the adsorptive removal of anionic pollutants in water (Goh et al., 2008). Over the past decades, LDHs have been extensively investigated as adsorbents for the treatment of various waterborne contaminants, such as dyes, monoatomic anions (e.g., fluoride), and oxyanions (e.g., arsenate, phosphate) (Seida and Nakano, 2002; Goh et al., 2009; Zhang et al., 2012; Deng et al., 2018). A few pioneering studies have reported the development of LDHs for PFOS and PFOA removal with a primary focus on the examination of the role of exchangeable anion composition (Hu et al., 2017; Chang et al., 2019; Alonso-de-Linaje et al., 2021; Chen et al., 2021). Specifically, nitrate-intercalated Mg–Al LDH has shown substantially better performance than carbonate-intercalated Mg–Al LDH for PFOS and PFOA adsorption (Hu et al., 2017; Alonso-de-Linaje et al., 2021). It has also been found that removal of carbonate from the interlayer of Mg–Al LDH substantially increased the adsorption of PFOA (Chang et al., 2019). Meanwhile, LDHs can exhibit varied cation compositions, but the effect of cation composition on PFAS adsorption remains unexplored. Additionally, while previous studies have primarily focused on PFOS and PFOA, the performance of LDHs for the removal of other PFAS is insufficiently understood.

In this study, we synthesized, characterized, and systematically compared the performance of two representative LDHs with different cation compositions, namely Mg–Al and Zn–Al LDHs, for PFAS removal. Nitrate-intercalated Mg–Al and Zn–Al LDHs were prepared because of the superior performance of nitrate compared to other intercalated anions (Hu et al., 2017). To our knowledge, this study investigated the performance of Zn–Al LDH for PFAS removal for the first time. PFOA was selected as a model anionic PFAS compound for detailed adsorption investigation due to its high environmental relevance (Post et al., 2009; Wang et al., 2017). Because of the shorter perfluoroalkyl moiety, PFOA generally showed less affinity than PFOS with many types of adsorbents (Du et al., 2014; Zhang et al., 2016; Dong et al., 2021). Additionally, the performance of the two LDHs were also evaluated for the removal of a suite of perfluorinated carboxylic acids (PFCAs) with different carbon chain lengths.

2. Materials and methods

2.1. Chemicals

Magnesium nitrate hexahydrate ($Mg(NO_3)_2\bullet 6H_2O$, Fisher Scientific), zinc nitrate hexahydrate ($Zn(NO_3)_2\bullet 6H_2O$, Alfa Aesar), aluminum nitrate nonahydrate ($Al(NO_3)_3\bullet 9H_2O$, EMD-Millipore), sodium hydroxide (NaOH, Fisher Scientific), hydrochloric acid (HCl, VWR-BDH), sodium bicarbonate ($NaHCO_3$, Fisher Scientific), sodium chloride (NaCl, Fisher Scientific), sodium sulfate decahydrate ($Na_2SO_4\bullet 10H_2O$, Fisher Scientific), and sodium nitrate ($NaNO_3$, Fisher Scientific) were used as purchased without further purification. Suwannee River Natural Organic Matter (NOM) was purchased from the International Humic Substances Society and was used to prepare a stock solution of 300 mg C/L with the calibration of a TOC analyzer (Shimadzu). Perfluorobutanoic acid (PFBA, Sigma-Aldrich), perfluoroheptanoic acid (PFHpA, Sigma-Aldrich), PFOA (Alfa Aesar), perfluorononanoic acid (PFNA, Sigma-Aldrich), and perfluorododecanoic acid (PFDoA, Oakwood Chemical) were used as representative PFCAs. Properties of the PFCAs were listed in Supplementary Material (Table S1 of Supplementary Material). Ultrapure water (resistivity >18.2 MΩ) was used to prepare solutions.

2.2. Preparation of Zn–Al and Mg–Al LDHs

Zn–Al and Mg–Al LDHs were selected as two model LDHs in the present work because they were commonly applied for the removal of anionic pollutants (You et al., 2001; Goh et al., 2008). Our preliminary experiments also showed that Zl-Al and Mg–Al LDHs had best performance for PFOA removal among a series of LDHs with different cation compositions (Fig. S1 of Supplementary Material). Zn–Al and Mg–Al LDHs were synthesized based on a slight modification of an aqueous co-precipitation approach reported elsewhere (Hu et al., 2017). For Zn–Al LDH, 100 mL of a mixed solution containing 0.75-M Zn $(NO_3)_2\bullet 6H_2O$ and 0.25-M $Al(NO_3)_3\bullet 9H_2O$ was prepared with the molar ratio $Zn^{2+}/Al^{3+} = 3{:}1$. The mixed salt solution was added into 100 mL of a 2-M NaOH solution under vigorous stirring in a dropwise manner. After completion of the reaction, the white slurry was aged at room temperature for 24 h and then centrifuged to collect the solids. The solids were washed with water several times to remove impurities and dried in air at 60 °C. The obtained solids were grinded to powders and stored for future use. Mg–Al LDH was synthesized following the same approach with the use of $Mg(NO_3)_2\bullet 6H_2O$ (0.75 M) and $Al(NO_3)_3\bullet 9H_2O$ (0.25 M) as precursors.

2.3. Material characterization

The morphology of the LDHs was determined using a Hitachi S-4800 scanning electron microscope (SEM). The crystalline structure of the LDHs was determined by powder X-ray diffraction (XRD) using Bruker D8 Discover A25 diffractometer with copper Kα radiation with a scan speed of 6° per min and a step size of 0.02°. The Brunauer−Emmett−-Teller (BET) surface area of the LDHs was determined based on $N_{2(g)}$ adsorption/desorption measurement using a Micromeritics ASAP 2020 Accelerated Surface Area and Porosimetry System. Zeta potential measurements of the LDHs were performed under pH 3–11 using a Malvern Zetasizer Nano ZS 90. Fourier-transform infrared spectroscopy (FTIR) measurements were acquired on a Shimadzu IRTracer100 Spectrometer. The vibrations corresponding to the wavenumbers ranging from 500 to 4000 cm^{-1} were collected with a resolution of 4 cm^{-1}. The thermo-gravimetric analysis (TGA) was conducted on a Discovery SDT 650 thermo-gravimeter (TA Instruments) in a 50-mL/min air flow. The temperature ranged from 30 to 800 °C and the heating rate was 10 °C/min. The anion exchange capacity of the LDHs was determined by immersing 25 mg of the Zn–Al or Mg–Al LDH in 25 mL of a 4-mM Na_2SO_4 solution at ambient temperature for 24 h. The solution after immersion was filtered through a 0.22-μm polyethersulfone (PES) syringe filter (Millipore), and nitrate concentration in the filtrate was measured by ion chromatography (IC) with suppressed conductivity detection (Dionex ICS-1000) (Ishikawa et al., 2007; Olfs et al., 2009).

2.4. Adsorption experiments

PFOA adsorption experiments were performed under batch mode at ambient temperature (22 ± 2 °C). Experiments were conducted using polypropylene reactors placed on an orbital shaker (Thermo Scientific) at 300 rpm at pH 6 with a PFOA concentration of 10 mg/L and an adsorbent loading of 0.25 g/L, unless otherwise specified. The relatively high PFOA concentration was used to fully investigate the different adsorption behaviors of Zn–Al and Mg–Al LDHs under various water chemistry conditions, and was within the range of PFOA concentrations used in previous batch adsorption studies (Yu et al., 2009; Chang et al., 2019; Alonso-de-Linaje et al., 2021). Notably, in some cases PFAS concentrations in contaminated groundwater near the source zone were reported as high as mg/L (Schultz et al., 2004). Adsorption kinetics studies were performed by collecting samples in a series of time intervals up to 24 h. Adsorption isotherm experiments were carried out with PFOA concentrations in the range of 10–300 mg/L to determine the maximum PFOA adsorption capacities onto the LDHs. Samples were collected after 24 h to ensure that adsorption reached equilibrium. Additionally, the effect of pH on PFOA adsorption was examined in a range of initial solution pH values (i.e., 3–11). The effect of common anions on PFOA adsorption was determined in the presence of 1 mM of chloride, nitrate, sulfate, or carbonates (predominantly as bicarbonate and carbonic acid under the experimental condition). The effect of ionic strength was determined using NaCl solutions with varied concentrations (1–50 mM). The effect of NOM was studied using Suwannee River NOM with concentrations ranging from 0.1 to 1 mM as C. Furthermore, a separate set of experiments were performed in single-solute solutions containing 10 mg/L of PFBA (C4), PFHpA (C7), PFNA (C9), or PFDoA (C12) to investigate the adsorption of various PFCAs with different carbon chain lengths. Each experimental condition was run in duplicates.

Reuse of Zn–Al LDH was evaluated by performing PFOA adsorption/regeneration experiments for three consecutive cycles. In each cycle, adsorption experiment was first conducted at pH 6 with a PFOA concentration of 10 mg/L and an adsorbent loading of 0.25 g/L. After 24 h of contact time, PFOA-loaded Zn–Al LDH was collected by centrifugation and then added into 20 mL of fresh methanol (i.e., one-time use) for 24 h under shaking for adsorbent regeneration.

2.5. PFCA measurement

Samples collected in all experiments were immediately filtered using 0.22-μm PES syringe filters (Millipore) to remove the adsorbents. Concentrations of PFOA or other PFCAs in the filtrates were analyzed using a high-performance liquid chromatography (HPLC, UltiMate 3000, Thermo Scientific) couple with single quadrupole mass spectrometry (ISQ EM, Thermo Scientific). Chromatography was performed using a C18 column (Acclaim™ 3 μm, 120 Å, 100 × 2.1 mm, Thermo Scientific). The mobile phase consisted of (A) Milli-Q water and (B) acetonitrile (Optima LCMS grade, Fisher Scientific), both amended with 0.1% formic acid (Fisher Scientific). The gradient of mobile phase started at 50% B, jumped to 90% B at 3 min, reversed to the original condition at 4.5 min, and maintained to 8 min at a flow rate of 400 μL/min. Mass spectrometry (MS) analysis was performed using the single quadrupole MS with an ESI source operated at negative mode with the following operating conditions: vaporizer temperature 227 °C, ion transfer tube temperature 300 °C, source voltage −2046 V, source current 0.88 μA; sheath gas pressure 42.9 psig, aux gas pressure 4.8 psig, and sweep gas pressure 0.5 psig.

The PFCA adsorption amount onto LDHs at equilibrium was calculated using Eq. 1, and the PFCA removal efficiency was calculated using Eq. 2:

$$q_e = \frac{(c_0 - c_e)^* V}{m} \#(1)$$

$$Removal\ (\%) = \left(1 - \frac{c_e}{c_0}\right) \times 100\% \#(2)$$

where q_e (mg/g) is the amount of PFCA adsorbed onto adsorbent at equilibrium, c_0 (mg/L) is the initial concentration of PFCA in solution, c_e (mg/L) is the concentration of PFCA in solution at equilibrium, m (g) is the mass of adsorbent, and V (L) is the volume of the PFCA solution.

3. Results and discussion

3.1. Characterization of synthesized LDHs

The structural and compositional properties of the as-synthesized LDHs were determined using a series of tools. Zn–Al and Mg–Al LDHs exhibited distinct and different morphologies. As shown in Fig. 1, Zn–Al LDH consisted of small thin flakes randomly stacked into larger clutters, while Mg–Al LDH was present as bulk material with thick laminar layers. A higher specific surface area was observed for Zn–Al LDH (3.7 m^2/g) than Mg–Al LDH (0.7 m^2/g), which was consistent with the smaller primary particle size of Zn–Al LDH. The layered structure of the synthesized LDHs was confirmed by the strong peaks at 2θ of ~10° that represented the (003) reflection of the LDHs (Fig. 2a). Based on the Bragg equation, the basal spacings (d_{003}) of Zn–Al and Mg–Al LDHs were calculated as 0.87 nm and 0.80 nm, respectively. The thickness of one brucite-like structural sheet was generally considered ~0.48 nm (Goh et al., 2008), and thus the interlayer distances of Zn–Al and Mg–Al LDHs were estimated as ~0.39 nm and ~0.32 nm, respectively. The slightly different interlayer distances might be related to the different interactions between nitrate and Zn–Al or Mg–Al structural layers (Seftel et al., 2008; Yang et al., 2014). Additionally, the peaks at 2θ of ~21°, 34°, 39°, 46°, and 61° were referred to the (006), (012), (015), (018), and (110) reflections of the LDHs (Hu et al., 2017). The result suggested that no crystalline phases other than the LDHs formed in the present study.

The functional groups of the LDHs were investigated using FTIR. For both Zn–Al and Mg–Al LDHs, the broad absorption peak at 3600-3200 cm^{-1} that was related to the metal-OH stretching indicated the abundance of hydroxyl groups within the LDH structure (Fig. 2b) (Zhang et al., 2017). The intensive band at ~1350 cm^{-1} may be assigned to the

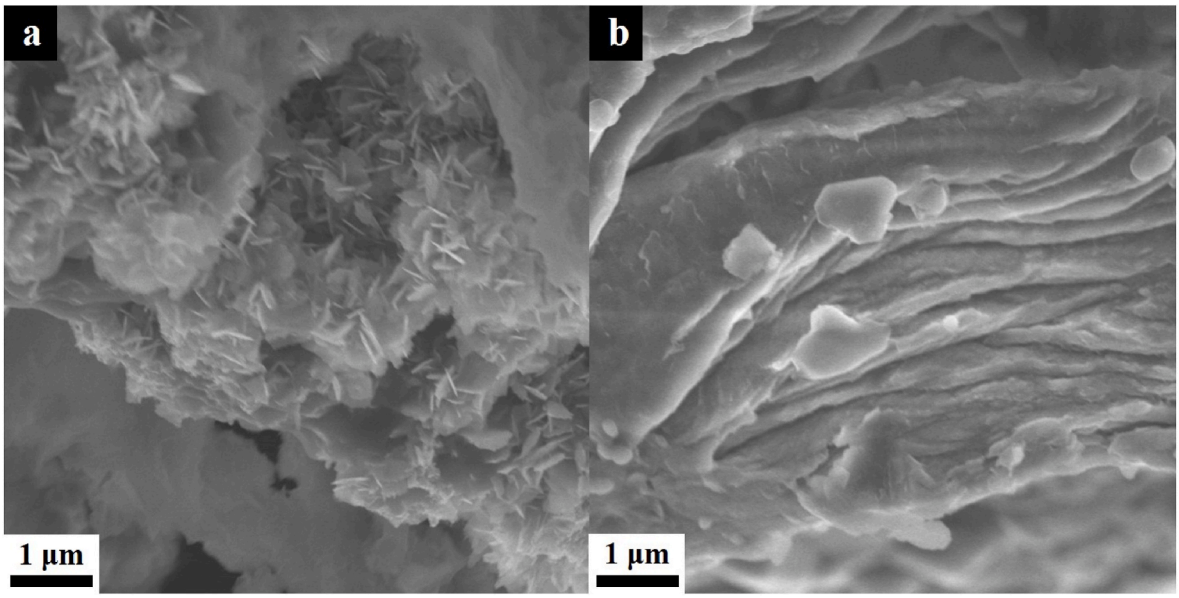

Fig. 1. SEM images of (a) Zn–Al and (b) Mg–Al LDHs.

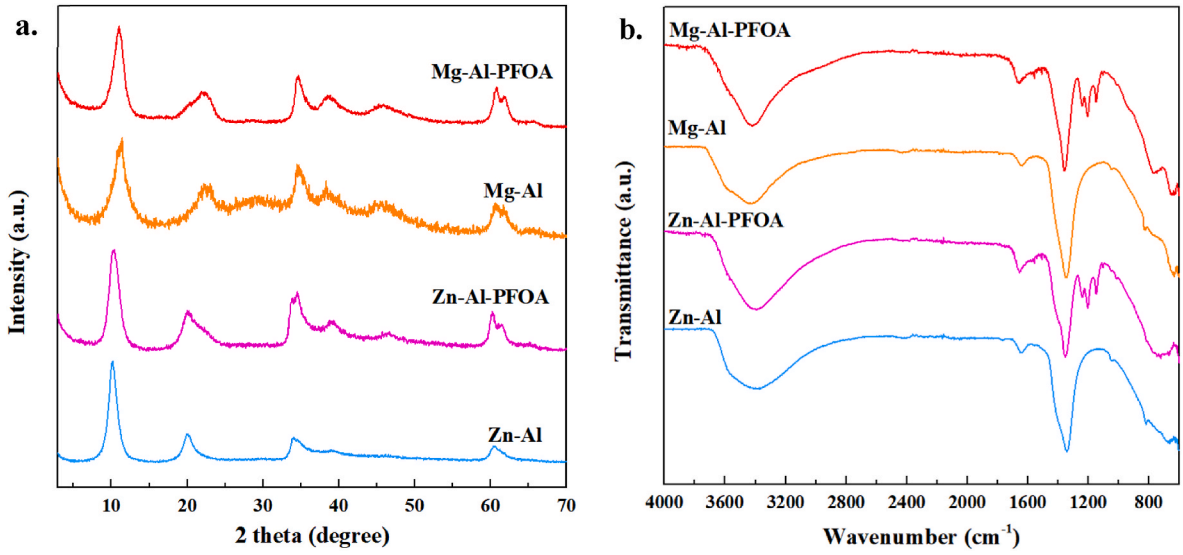

Fig. 2. (a) XRD patterns and (b) FTIR spectra of Zn–Al and Mg–Al LDHs before and after PFOA adsorption.

vibrations of the nitrate ion (Olfs et al., 2009; Hu et al., 2017), and the small peak centered at ~1640 cm^{-1} corresponded to the bending vibration of adsorbed H_2O (Chuang et al., 2008). Based on the TGA analysis, the gradual weight loss of the LDHs at up to ~200 °C represented the removal of water adsorbed within the interlayer as well as on the external surface of the LDHs (Fig. S2 of Supplementary Material) (Seftel et al., 2008). The weight loss at higher temperature (~200–~500 °C) was due to the dihydroxylation of the LDH structural layers and decomposition of the nitrate anions (Theiss et al., 2013; Yang et al., 2019, 2020a). Minimal weight loss was observed above 500 °C, suggesting the conversion of LDHs to (mixed) metal oxides.

The surface charges of Zn–Al and Mg–Al LDHs were determined based on zeta potential measurements at pH 3–11. In general, the zeta potentials decreased with increasing pH for both Zn–Al and Mg–Al LDHs (Fig. 3). Compared to Mg–Al LDH, Zn–Al LDH had higher positive zeta potentials at pH 3–9. However, Zn–Al LDH became negatively charged at pH 11, while the zeta potential of Mg–Al LDH remained positive at pH 11. Accordingly, the point of zero charge (pH_{pzc}) values for Zn–Al and Mg–Al LDHs were ~10 and > 11, respectively. The pH_{pzc} values of LDHs depended on the cation and anion composition of the materials, and have been reported in the range of 7.2–12.5 for LDHs with varied compositions (Goh et al., 2008). Overall, both Zn–Al and Mg–Al LDHs would be positively charged under circumneutral and slightly basic conditions relevant to water and wastewater treatment.

3.2. Adsorption kinetics and isotherms of PFOA

The adsorption behavior of PFOA onto Zn–Al and Mg–Al LDHs was determined using adsorption kinetics and isotherm studies. The kinetics experiments found that both Zn–Al and Mg–Al LDHs showed a rapid PFOA uptake initially, followed by a gradually slower stage until the adsorption equilibrium was achieved (Fig. 4). Notably, Zn–Al LDH rapidly removed ~95% PFOA in solution within 1 h, and >98% PFOA removal was achieved when adsorption reached equilibrium within 2 h. Meanwhile, the equilibrium state was achieved after 8 h with the use of Mg–Al LDH with the PFOA removal efficiency reaching ~66% at

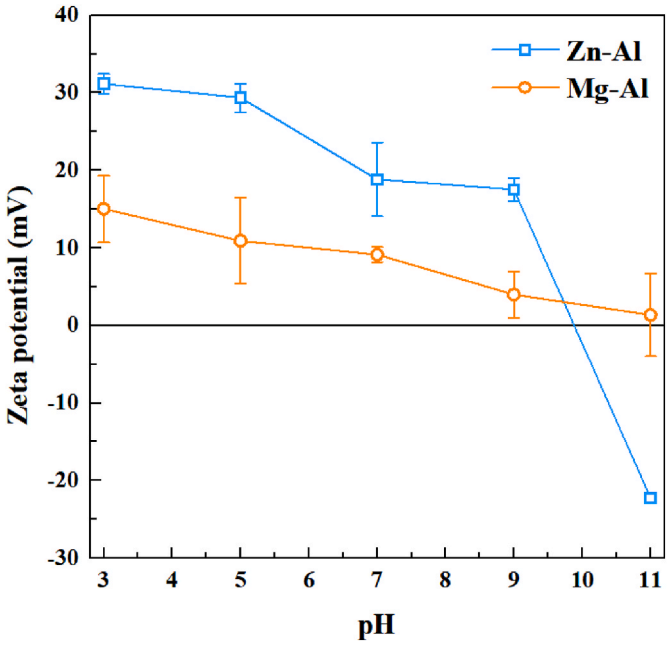

Fig. 3. Zeta potentials of Zn–Al and Mg–Al LDHs at pH 3–11.

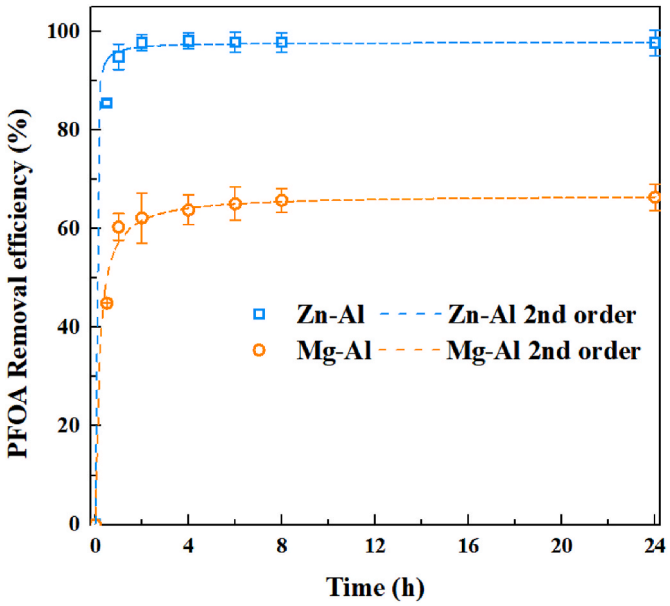

Fig. 4. Adsorption kinetics of PFOA onto Zn–Al and Mg–Al LDHs at pH 6 with an initial PFOA concentration of 10 mg/L and an adsorbent loading of 0.25 g/L. Dash lines represent pseudo-second order model fits.

equilibrium. The higher PFOA removal efficiency using Zn–Al LDH may suggest its stronger affinity with PFOA than that of Mg–Al LDH. Our observation was also consistent with previous studies using LDHs with various anion compositions showing that the equilibration time for PFOA adsorption was in the range of 1–8 h (Chang et al., 2019; Alonso-de-Linaje et al., 2021; Chen et al., 2021). For comparison, PFOA adsorption by powdered activated carbon (PAC) generally took several hours to reach equilibrium, and it may take several days for PFOA adsorption to reach equilibrium by GAC and ion exchange resin (Yu et al., 2009; Zhang et al., 2016; Dixit et al., 2021). While the adsorption kinetics may be affected by experimental factors such as adsorbent and adsorbate concentrations (Du et al., 2014), LDHs generally exhibited fast PFOA adsorption kinetics comparable to PAC, and were substantially faster than GAC and ion exchange resin.

The PFOA adsorption kinetics onto Zn–Al and Mg–Al LDHs were fitted to the pseudo-second order model, with the linearized form described in Eq. 3:

$$\frac{t}{q_t} = \frac{1}{k_2 q_e^2} + \frac{t}{q_e} \quad \#(3)$$

where t (h) is the contact time, q_e (mg/g) and q_t (mg/g) are the amount of PFOA adsorbed at equilibrium and at time t, respectively, and k_2 (g/(mg·h)) is the rate constant for pseudo-second order adsorption process. Based on the fitting result (Fig. S3 of Supplementary Material), the pseudo-second order model was suitable to describe the PFOA adsorption kinetics onto both Zn–Al and Mg–Al LDHs, which indicated that the adsorption rate was related to the number of available sites of the adsorbent (Ho and McKay, 1999). Specifically, the fitted rate constant of Zn–Al LDH was ~6 times higher than Mg–Al LDH (Table S2 of Supplementary Material), which was consistent with its much shorter contact time for PFOA adsorption to reach equilibrium. The substantially faster PFOA adsorption kinetics using Zn–Al LDH than Mg–Al LDH may be due to the higher surface area and smaller particle size of Zn–Al LDH that provided more available sites for adsorption. Additionally, Zn–Al LDH had a slightly larger basal spacing than Mg–Al LDH, which might make the adsorption sites within the interlayer more accessible by PFOA and thus favor the overall adsorption kinetics.

The adsorption capacities of PFOA onto Zn–Al and Mg–Al LDHs were compared based on equilibrium adsorption isotherm experiments (Fig. 5), and the data were fitted with both the classic Langmuir and Freundlich models, as given in Eqs. (4) and (5), respectively (Foo and Hameed, 2010).

$$q_e = \frac{q_{max} K_L c_e}{1 + K_L c_e} \quad \#(4)$$

$$q_e = K_F c_e^{\frac{1}{n}} \quad \#(5)$$

where q_e (mg/g) is the amount of PFOA adsorbed at equilibrium, c_e (mg/L) is the equilibrium PFOA concentration in the solution, K_L (L/mg) is the Langmuir constant related to the energy of adsorption, q_{max} (mg/g) is the Langmuir adsorption capacity, K_F ((mg/g)·(L/mg)$^{1/n}$) is the

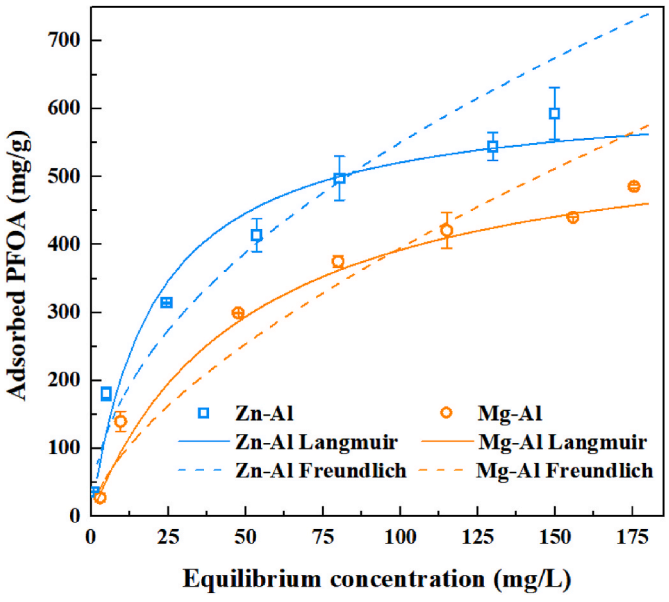

Fig. 5. Adsorption isotherms of PFOA onto Zn–Al and Mg–Al LDHs at pH 6 with an adsorbent loading of 0.25 g/L. Solid and dash lines represent Langmuir and Freundlich model fits, respectively.

Freundlich constant denoting the adsorption affinity, and n is a dimensionless indicator related to the adsorption heterogeneity.

Overall, the Langmuir model fitted the PFOA adsorption data slightly better than the Freundlich model for both Zn–Al and Mg–Al LDHs (Table S3 of Supplementary Material). On the basis of the Langmuir model, the K_L value for Zn–Al LDH was ~2.5 times compared to Mg–Al LDH, indicating that the adsorption affinity between PFOA and Zl-Al LDH was substantially stronger than that of Mg–Al LDH. This result was consistent with the higher PFOA removal efficiency using Zn–Al LDH than Mg–Al LDH shown in the kinetics study (Fig. 4). The Langmuir adsorption capacities of PFOA were obtained as 625 mg/g (1.51 mmol/g) and 588 mg/g (1.42 mmol/g) for Zn–Al LDH and Mg–Al LDH, respectively. These values were substantially higher than many carbonaceous materials, as well as advanced adsorbents such as organic-modified clays and metal organic framework (MOF) reported in literature (Table S4 of Supplementary Material) (Yu et al., 2009; Chen et al., 2017; Yang et al., 2020b; Dong et al., 2021; Wang et al., 2021). Specifically, the PFOA adsorption capacities for Zn–Al and Mg–Al LDHs were about twice as high as commercial PAC, and several times higher than GAC (Yu et al., 2009; Zhang et al., 2016).

It should be noted that while the PFOA adsorption capacity for Zn–Al LDH was slightly higher than Mg–Al LDH, both values were much lower than their corresponding anion exchange capacities (i.e., measured as 2.30 meq/g for Zn–Al LDH and 3.35 meq/g for Mg–Al LDH), which indicated that not all sites within the interlayers of the Zn–Al and Mg–Al LDHs were accessible for adsorption because of the confined space. Previous research found that calcination of carbonate-intercalated Mg–Al LDH distorted the layered structure and thus substantially increased the PFOA adsorption capacity (Chang et al., 2019). Interestingly, after calcination, the PFOA adsorption capacity reported in that study was higher than the anion exchange capacity of the LDH, which may be related to the micelle/hemimicelle formation of PFOA molecules onto the LDH because of the high PFOA concentrations (up to 3000 mg/L) (Chang et al., 2019). It has been reported that the type of intercalated anions strongly affected PFAS adsorption capacities for LDHs (Hu et al., 2017; Alonso-de-Linaje et al., 2021). The present study suggested that PFOA adsorption behavior may also be dependent on the cation composition of LDHs. Compared to Mg–Al LDH, Zn–Al LDH showed stronger affinity with PFOA, which might be related to its higher surface charge under circumneutral conditions (Fig. 3) that provided stronger electrostatic interactions with PFOA anions than that of Mg–Al LDH.

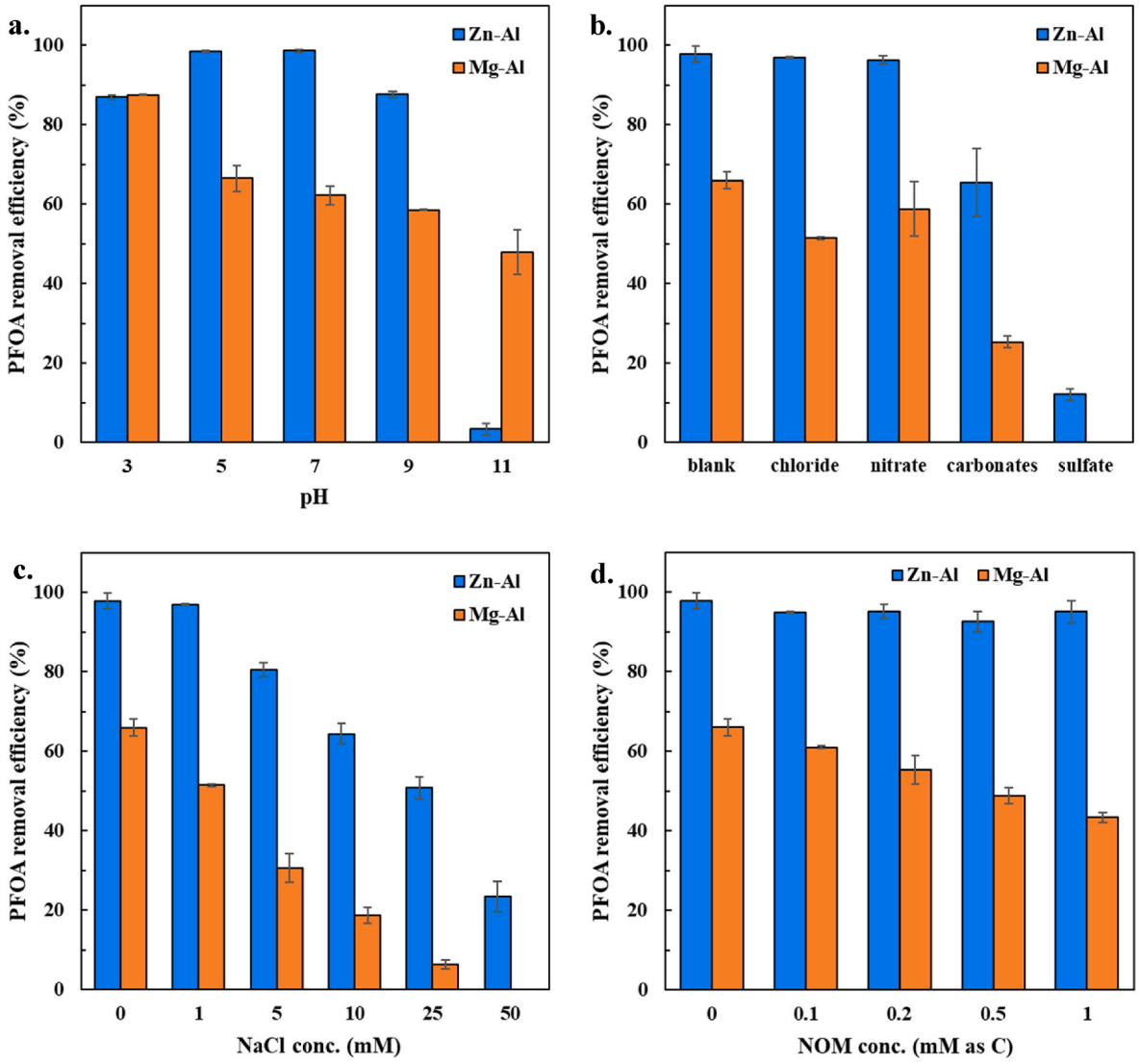

Fig. 6. Effect of (a) solution pH, (b) inorganic anions (1 mM), (c) ionic strength, and (d) NOM on PFOA adsorption onto Zn–Al and Mg–Al LDHs with an initial PFOA concentration of 10 mg/L and an adsorbent loading of 0.25 g/L (b), (c) and (d) were conducted at pH 6.

3.3. Effect of water chemistry parameters

The performance of Zn–Al and Mg–Al LDHs for PFOA removal was evaluated under various water chemistry conditions. PFOA adsorption onto Zn–Al and Mg–Al LDHs was affected by solution pH, and PFOA removal efficiency generally decreased with increasing pH under the experimental conditions (Fig. 6a). For Zn–Al LDH, >98% PFOA removal was observed at pH 5–7, and increasing the solution pH to 9 slightly reduced PFOA removal efficiency. However, PFOA removal efficiency dropped sharply to <5% when the solution pH further increased to 11, which may be related to the change of the surface charge of Zn–Al LDH. Because of the low pK_a, PFOA would be present in its deprotonated form at pH 3–11 (Fig. S4 of Supplementary Material) (Zhang et al., 2019). Thus, the positive surface charge of Zn–Al LDH at pH 3–9 would favor the adsorption of PFOA through electrostatic interactions. It should be noted that a slightly lower PFOA removal efficiency was observed at pH 3 than 5 and 7, probably because the stability of Zn–Al LDH structure may be impaired at low pH which consequently decreased PFOA adsorption (Goh et al., 2008). In contrast, the surface of Zn–Al LDH became negatively charged at pH 11 (Fig. 3), which would induce electrostatic repulsion with the PFOA anions, resulting in the dramatic decrease of PFOA removal. Compared to Zn–Al LDH, Mg–Al LDH exhibited lower PFOA removal efficiency at pH 5–9; meanwhile, ~50% PFOA removal was observed at pH 11 using Mg–Al LDH, which was substantially higher than using Zn–Al LDH and may be related to the positive surface charge of Mg–Al LDH at pH 11 (Fig. 3).

Chloride, carbonates, nitrate and sulfate are among major anions commonly present in water sources (Drever, 1988), and their effects on PFOA adsorption onto Zn–Al and Mg–Al LDHs were evaluated. For Zn–Al LDH, the presence of 1 mM of chloride and nitrate had no impact on PFOA removal; however, PFOA removal efficiency was moderately reduced to ~65% in the presence of carbonates, and the presence of sulfate severely inhibited PFOA adsorption (Fig. 6b). Similar trend was observed for Mg–Al LDH, and the anions showed stronger inhibitory effects on PFOA adsorption onto Mg–Al LDH than Zn–Al LDH (Fig. 6b). Both Zn–Al and Mg–Al LDHs were quite hydrophilic (Fig. S5 of Supplementary Material), and thus PFOA adsorption onto Zn–Al and Mg–Al LDHs may probably be mainly through electrostatic interactions. The negative charge of PFOA in aqueous solution may come from both the carboxylate functional group and the unique molecular structure (Johnson et al., 2007). Specifically, because of the high electronegativity of fluorine atoms, the perfluoroalkyl chain of PFOA may also carry a partial negative charge (Xiao et al., 2011). Thus, PFOA may have a stronger binding affinity with LDHs than that of the monovalent nitrate and chloride, and be more preferentially adsorbed onto LDHs. Meanwhile, the moderate inhibition of carbonates may be related to the specific metal-carbonates interactions that affected the adsorption sites (Goh et al., 2008; Mishra et al., 2018). The strong inhibitory effect of sulfate was consistent with the stronger binding affinity of divalent anions than monovalent anions with positively charged adsorbent through electrostatic attraction (Benjamin, 2002; Min et al., 2020). It has been reported that sulfate reduced the adsorption of PFOS and chlorinated polyfluoroalkyl ether sulfonate (F–53B) onto Mg–Al LDH by ~70% and ~50%, respectively (Hu et al., 2017; Ding et al., 2020). Previous research also found that the adsorption of selenite (i.e., an inorganic anion) onto Mg–Al LDH was inhibited by competing anions in the order that sulfate > carbonates > nitrate (You et al., 2001). Notably, the strong inhibitory effect of sulfate on PFOA adsorption in the present work may be mitigated with the use of higher adsorbent loadings. For instance, when the Zn–Al LDH loading increased from 0.25 to 2 g/L, PFOA removal efficiency increased from ~10% to >80% in the presence of sulfate, which may likely be attributed to the presence of more adsorption sites to capture PFOA (Fig. S6 of Supplementary Material).

The important role of electrostatic interactions in PFOA adsorption was further investigated by performing the adsorption experiments under a series of ionic strengths. An increase of ionic strength gradually reduced PFOA removal efficiency using both Zn–Al and Mg–Al LDHs (Fig. 6c), which may be attributed to the compression of the electrical double layer under high ionic strengths that would reduce the electrostatic attraction between PFOA and the positively charged LDHs (Min et al., 2020). This observation suggested that PFOA adsorption onto Zn–Al and Mg–Al LDHs may primarily rely on electrostatic interactions. Compared to Mg–Al LDH, the increase of ionic strength had a less inhibitory effect on PFOA adsorption onto Zn–Al LDH, which may be related to the higher positive surface charge of Zn–Al LDH under the experimental condition that resulted in a stronger affinity with PFOA than that of Mg–Al LDH (Fig. 3). Similarly, a recent study also reported that increased ionic strengths dramatically reduced PFOA adsorption onto Cu–Mg–Fe LDH (Chen et al., 2021).

NOM is a complex organic matrix with ubiquitous presence in natural waters (Matilainen et al., 2011). The effect of NOM on PFOA adsorption onto Zn–Al and Mg–Al LDHs was evaluated using Suwannee River NOM ranging from 0.1 to 1 mM as C. As shown in Fig. 6d, the presence of up to 1 mM of NOM had no inhibitory effect on PFOA removal by Zn–Al LDH. Meanwhile, increasing NOM concentrations mildly reduced PFOA removal by Mg–Al LDH, and the extent of inhibition at 1 mM of NOM was comparable to that at 1 mM of NaCl. NOM generally carries negative charges under circumneutral conditions and has been reported to inhibit PFAS adsorption onto numerous classes of adsorbents such as activated carbon and ion exchange resin (Gagliano et al., 2020; Boyer et al., 2021). Given the hydrophilic nature of Mg–Al LDH, the minor inhibitory effect of NOM may be attributed to its competition with PFOA for adsorption sites onto Mg–Al LDH through electrostatic but not hydrophobic interactions, although other mechanism such as pore blockage cannot be fully excluded. Compared to Mg–Al LDH, the robust performance of Zn–Al LDH in the presence of NOM may indicate its stronger adsorption affinity with PFOA than that of Mg–Al LDH.

3.4. Adsorption of PFCAs

The performance of Zn–Al and Mg–Al LDHs was compared for the removal of five PFCAs with various carbon chain lengths, including PFBA, PFHpA, PFOA, PFNA and PFDoA. All of the five PFCAs are in the proposed fifth Unregulated Contaminant Monitoring Rule (UCMR5) by the U.S. EPA (EPA, 2021), and PFHpA, PFOA and PFNA were also previously listed under the U.S. EPA UCMR3 (EPA, 2012). Overall, the PFCA removal efficiency generally increased with increasing chain lengths of their perfluoroalkyl moiety. Specifically, nearly complete removal of PFDoA was observed using both Zn–Al and Mg–Al LDHs. For PFNA, PFOA and PFHpA, Zn–Al LDH exhibited better performance than Mg–Al LDH with the removal efficiency reaching >95%; in contrast, the removal efficiencies of these three PFCAs were in the range of ~50–90% with the use of Mg–Al LDH. Meanwhile, both materials showed comparable and relatively low (i.e., ~50%) PFBA removal efficiency (Fig. 7). Compared with Mg–Al LDH, the overall better performance of Zn–Al LDH may be attributed to its higher surface charge under the experimental condition and the slightly larger basal spacing that made the adsorption sites more readily accessible.

It is generally accepted that the hydrophobicity of PFAS increased with increasing perfluoroalkyl chain lengths (Higgins and Luthy, 2006; Park et al., 2020b). Thus, longer-chain PFAS exhibited stronger affinity with numerous carbonaceous materials (Zhang et al., 2019; Park et al., 2020b), while adsorption of shorter-chain PFAS such as PFBA has been recognized as a unique challenge because of the weak adsorbent-adsorbate interactions (Li et al., 2020; Vu and Wu, 2020). Interestingly, although electrostatic interactions were likely the main driving force for PFCA adsorption onto LDHs, we observed a similar trend that the removal efficiency depended on the perfluoroalkyl chain length of the PFCAs in the present work. The better removal of longer-chain PFCAs by LDHs may be related to their increased anionic characters in comparison to shorter-chain PFCAs (Boyer et al., 2021).

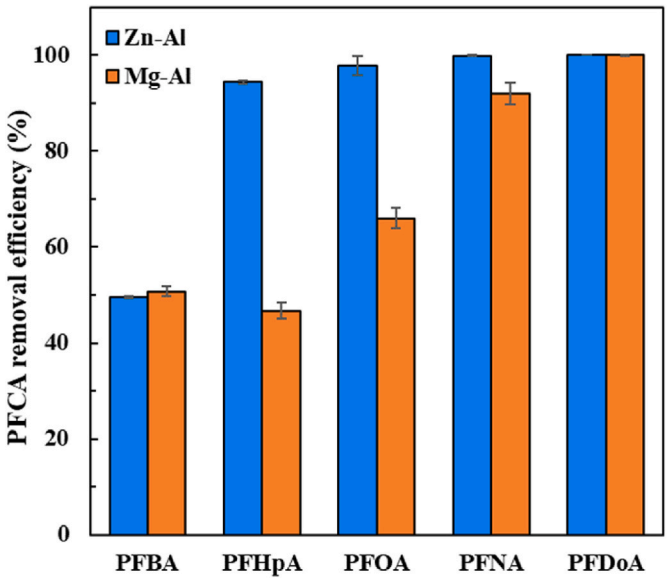

Fig. 7. Adsorption of different PFCAs onto Zn–Al and Mg–Al LDHs at pH 6 with an initial PFCA concentration of 10 mg/L and an adsorbent loading at 0.25 g/L.

Based on density functional theory calculations, it has been suggested that the total negative atomic charge increased with the increasing lengths of perfluoroalkyl moiety of PFCAs, thereby causing stronger electrostatic interactions between long-chain PFCAs and adsorbent surface (Park et al., 2020a).

3.5. LDH regeneration and reuse

Reusability of adsorbent is important and valuable in practical water and wastewater treatment applications. Since Zn–Al LDH showed better performance for PFOA adsorption than Mg–Al LDH, the reusability of Zn–Al LDH for PFOA removal was evaluated by performing the adsorption/regeneration experiments for three cycles with the use of methanol to regenerate the PFOA-loaded Zn–Al LDH in each cycle (Du et al., 2016; Gagliano et al., 2020). Notably, regeneration did not compromise the performance of Zn–Al LDH, and >98% removal of PFOA was observed for all three cycles (Fig. S7 of Supplementary Material). The result suggested that Zn–Al LDH may be an efficient and robust adsorbent that can be used for multiple times for PFOA removal applications.

3.6. Characterization of LDHs after PFOA adsorption

XRD was employed to characterize Zn–Al and Mg–Al LDHs after PFOA adsorption experiments (i.e., 10 mg/L PFOA, 0.25 g/L adsorbent dosage). Compared to raw Zn–Al and Mg–Al LDHs, no substantial changes were observed in the XRD patterns of the Zn–Al and Mg–Al LDHs after PFOA adsorption (Fig. 2a), suggesting that the LDHs were stable without changing any crystalline structures during PFOA adsorption process. For both Zn–Al and Mg–Al LDHs, the minimal shift of the (003) reflection peak at 2θ of ~10° indicated that PFOA adsorption did not alter the basal spacings of the LDHs, which may be attributed to the strong interlayer interactions between adjacent sheets of LDHs as well as the relatively low PFOA loading onto the LDHs under the experimental condition (i.e., <4 wt%). Previous research reported that adsorption of μM level of PFOA and PFOS did not alter the basal spacing of Cu–Mg–Fe LDH (Chen et al., 2021), which was consistent with our observation for Zn–Al and Mg–Al LDHs. Similarly, Chang et al. (2019) investigated PFOA adsorption onto calcined Mg–Al LDH under high PFOA concentrations (200–3000 mg/L), and found that the basal spacing of calcined Mg–Al LDH only started to increase when PFOA concentrations were above 1000 mg/L. Compared to the swellable layered materials such as natural clays (e.g., montmorillonite), LDHs are more difficult to be expanded because of their high charge density and hydrophilic nature that lead to a tight stacking of the layers (Adachi-Pagano et al., 2000; Wang and O'Hare, 2012).

FTIR spectra confirmed that PFOA was retained within Zn–Al and Mg–Al LDHs. After PFOA adsorption, three new peaks at ~1145, 1210 and 1245 cm^{-1} were observed for both Zn–Al and Mg–Al LDHs (Fig. 2b), which were attributed to the vibrations of the $–CF_3$ and $–CF_2$- groups of adsorbed PFOA (Chen et al., 2017). The vibration of COO^- group was typically located at ~1660 cm^{-1} (Li et al., 2012), which could be largely overlapped with that of bending vibration of adsorbed H_2O and made it challenging to fully differentiate these two peaks. However, a small shift of the peak at ~1640 cm^{-1} to a higher wavenumber was observed for both Zn–Al and Mg–Al LDHs after PFOA adsorption (Fig. 2b), which might imply interactions between the positively charged structural layers of LDHs and the carboxylic group of PFOA. Overall, the characterization results, together with the hydrophilic character of LDHs and the inhibitory effect of ionic strengths and competing anions, suggested that electrostatic interactions may be the primary mechanism for PFOA adsorption onto Zn–Al and Mg–Al LDHs.

3.7. Practical considerations

Results of the present work suggested that LDHs may be an efficient adsorbent for PFAS removal. In practice, LDHs may be prepared in large scale from metal nitrate salts that are commonly used for agricultural and industrial applications. Based on the low cost of the raw materials, LDHs may potentially be a cost-effective alternative to conventional adsorbents such as activated carbon. LDHs may be prepared in powdered form and applied in a similar manner to PAC in *ex situ* water treatment applications. Previous research also reported the synthesis of granular LDHs (Sun et al., 2014), which made it possible to employ LDHs in column-type filters. Additionally, LDHs may potentially be used alone or mixed with other media as an amendment for *in situ* remediation of PFAS-contaminated soil and/or groundwater. To promote the application of LDHs, future research can be dedicated to (1) careful design of LDH-based materials with improved performance in the presence of competing anions, (2) systematic investigation of the effect of PFAS structures and functional groups on the adsorption onto LDHs (3) elucidation of the role of LDH structures (e.g., interlayer distance) in the accommodation and capture of different PFAS molecules, (4) further optimization of the LDH regeneration process, and (5) comprehensive evaluation of the removal of various PFAS structures under environmentally relevant settings.

4. Conclusions

In this research, nitrate-intercalated Zn–Al and Mg–Al LDHs were prepared, characterized, and systematically compared for the adsorption of PFOA as a representative PFAS. Compared with Mg–Al LDH, Zn–Al LDH showed higher adsorption capacity, stronger adsorption affinity, and faster adsorption kinetics for PFOA, which may be attributed to the higher surface charge, larger surface area, and slightly larger basal spacing of Zn–Al LDH that made the adsorption sites readily accessible. Additionally, Zn–Al LDH performed better than Mg–Al LDH for the removal of a series of PFCAs with varied chain lengths. The presence of NOM had minimal impact on PFOA removal, but sulfate as well as increased ionic strengths severely inhibited PFOA adsorption onto Zn–Al and Mg–Al LDHs. Our results suggested that PFOA adsorption onto LDHs may primarily rely on electrostatic interactions, and cation composition of LDHs can have significant effect on its performance for PFAS removal.

Credit author statement

Jingwan Huo: Conceptualization, Data curation, Formal analysis,

Methodology, Writing – original draft, Writing – review & editing. Xiaopeng Min: Data curation, Formal analysis, Methodology. Qianqian Dong: Data curation, Formal analysis, Methodology. Shangping Xu: Conceptualization, Funding acquisition, Writing – review & editing. Yin Wang: Conceptualization, Funding acquisition, Investigation, Methodology, Project administration, Supervision, Writing – original draft, Writing – review & editing.

Declaration of competing interest

The authors declare that they have no known competing financial interests or personal relationships that could have appeared to influence the work reported in this paper.

Acknowledgements

This work was supported by the National Science Foundation (NSF) Industry/University Cooperative Research Center on Water Equipment and Policy located at University of Wisconsin – Milwaukee (UWM, IIP-1540032). All opinions expressed in this work are the authors' and do not necessarily reflect the views of NSF. XRD and surface area analyses were performed at the Advanced Analysis Facility at UWM. FTIR, zeta potential, and TGA measurements were conducted in the Water Technology Accelerator at UWM. SEM was performed in the Department of Biology at UWM. We are grateful to the anonymous reviewers for their constructive comments that helped strengthen this paper.

Appendix A. Supplementary data

Supplementary data to this article can be found online at https://doi.org/10.1016/j.chemosphere.2021.132297.

References

Adachi-Pagano, M., Forano, C., Besse, J.P., 2000. Delamination of layered double hydroxides by use of surfactants. Chem. Commun. 91–92 https://doi.org/10.1039/A908251D.

Alonso-de-Linaje, V., Mangayayam, M.C., Tobler, D.J., Rives, V., Espinosa, R., Dalby, K. N., 2021. Enhanced sorption of perfluorooctane sulfonate and perfluorooctanoate by hydrotalcites. Environ. Technol. Innov. 21, 101231. https://doi.org/10.1016/j.eti.2020.101231.

Ateia, M., Alsbaiee, A., Karanfil, T., Dichtel, W., 2019. Efficient PFAS removal by amine-functionalized sorbents: critical review of the current literature. Environ. Sci. Technol. Lett. 6, 688–695. https://doi.org/10.1021/acs.estlett.9b00659.

Benjamin, M.M., 2002. Water Chemistry. McGraw-Hill, New York, NY.

Boyer, T.H., Fang, Y., Ellis, A., Dietz, R., Choi, Y.J., Schaefer, C.E., Higgins, C.P., Strathmann, T.J., 2021. Anion exchange resin removal of per-and polyfluoroalkyl substances (PFAS) from impacted water: a critical review. Water Res. 117244 https://doi.org/10.1016/j.watres.2021.117244.

Chang, P.H., Jiang, W.T., Li, Z., 2019. Removal of perfluorooctanoic acid from water using calcined hydrotalcite–A mechanistic study. J. Hazard Mater. 368, 487–495. https://doi.org/10.1016/j.jhazmat.2019.01.084.

Chen, W., Zhang, X., Mamadiev, M., Wang, Z., 2017. Sorption of perfluorooctane sulfonate and perfluorooctanoate on polyacrylonitrile fiber-derived activated carbon fibers: in comparison with activated carbon. RSC Adv. 7, 927–938. https://doi.org/10.1039/C6RA25230C.

Chen, Y., Georgi, A., Zhang, W., Kopinke, F.-D., Yan, J., Saeidi, N., Li, J., Gu, M., Chen, M., 2021. Mechanistic insights into fast adsorption of perfluoroalkyl substances on carbonate-layered double hydroxides. J. Hazard Mater. 408, 124815. https://doi.org/10.1016/j.jhazmat.2020.124815.

Chuang, Y.H., Tzou, Y.M., Wang, M.K., Liu, C.H., Chiang, P.N., 2008. Removal of 2-clorophenol from aqueous solution by Mg/Al layered double hydroxide (LDH) and modified LDH. Ind. Eng. Chem. Res. 47, 3813–3819. https://doi.org/10.1021/ie071508e.

Cousins, I.T., DeWitt, J.C., Glüge, J., Goldenman, G., Herzke, D., Lohmann, R., Ng, C.A., Scheringer, M., Wang, Z., 2020. The high persistence of PFAS is sufficient for their management as a chemical class. Environ. Sci.: Process. Impacts 22, 2307–2312. https://doi.org/10.1039/D0EM00355G.

Deng, L., Zeng, H., Shi, Z., Zhang, W., Luo, J., 2018. Sodium dodecyl sulfate intercalated and acrylamide anchored layered double hydroxides: a multifunctional adsorbent for highly efficient removal of Congo red. J. Colloid Interface Sci. 521, 172–182. https://doi.org/10.1016/j.jcis.2018.03.040.

Ding, D., Song, X., Wei, C., Hu, Z., Liu, Z., 2020. Efficient sorptive removal of F-53B from water by layered double hydroxides: performance and mechanisms. Chemosphere 252, 126443. https://doi.org/10.1016/j.chemosphere.2020.126443.

Dixit, F., Dutta, R., Barbeau, B., Berube, P., Mohseni, M., 2021. PFAS removal by ion exchange resins: a review. Chemosphere. https://doi.org/10.1016/j.chemosphere.2021.129777, 129777.

Dong, Q., Min, X., Huo, J., Wang, Y., 2021. Efficient sorption of perfluoroalkyl acids by ionic liquid-modified natural clay. Chem. Eng. J. Adv. 7, 100135. https://doi.org/10.1016/j.ceja.2021.100135.

Drever, J.I., 1988. The Geochemistry of Natural Waters. Prentice Hall, Englewood Cliffs.

Du, Z., Deng, S., Bei, Y., Huang, Q., Wang, B., Huang, J., Yu, G., 2014. Adsorption behavior and mechanism of perfluorinated compounds on various adsorbents—a review. J. Hazard Mater. 274, 443–454. https://doi.org/10.1016/j.jhazmat.2014.04.038.

Du, Z., Deng, S., Zhang, S., Wang, B., Huang, J., Wang, Y., Yu, G., Xing, B., 2016. Selective and high sorption of perfluorooctanesulfonate and perfluorooctanoate by fluorinated alkyl chain modified montmorillonite. J. Phys. Chem. C 120, 16782–16790. https://doi.org/10.1021/acs.jpcc.6b04757.

EPA, 2012. Third Unregulated Contaminant Monitoring Rule. https://www.epa.gov/dwucmr/third-unregulated-contaminant-monitoring-rule.

EPA, 2016. Drinking Water Health Advisory for Perfluorooctanoic Acid (PFOA). EPA Document 822-R-16-005.

EPA, 2021. Fifth Unregulated Contaminant Monitoring Rule. https://www.epa.gov/dwucmr/fifth-unregulated-contaminant-monitoring-rule.

Espana, V.A.A., Mallavarapu, M., Naidu, R., 2015. Treatment technologies for aqueous perfluorooctanesulfonate (PFOS) and perfluorooctanoate (PFOA): a critical review with an emphasis on field testing. Environ. Technol. Innov. 4, 168–181. https://doi.org/10.1016/j.eti.2015.06.001.

Foo, K.Y., Hameed, B.H., 2010. Insights into the modeling of adsorption isotherm systems. Chem. Eng. J. 156, 2–10. https://doi.org/10.1016/j.cej.2009.09.013.

Gagliano, E., Sgroi, M., Falciglia, P.P., Vagliasindi, F.G., Roccaro, P., 2020. Removal of poly-and perfluoroalkyl substances (PFAS) from water by adsorption: role of PFAS chain length, effect of organic matter and challenges in adsorbent regeneration. Water Res. 171, 115381. https://doi.org/10.1016/j.watres.2019.115381.

Goh, K.H., Lim, T.T., Dong, Z., 2008. Application of layered double hydroxides for removal of oxyanions: a review. Water Res. 42, 1343–1368. https://doi.org/10.1016/j.watres.2007.10.043.

Goh, K.H., Lim, T.T., Dong, Z., 2009. Enhanced arsenic removal by hydrothermally treated nanocrystalline Mg/Al layered double hydroxide with nitrate intercalation. Environ. Sci. Technol. 43, 2537–2543. https://doi.org/10.1021/es802811n.

Higgins, C.P., Luthy, R.G., 2006. Sorption of perfluorinated surfactants on sediments. Environ. Sci. Technol. 40, 7251–7256. https://doi.org/10.1021/es061000n.

Ho, Y.S., McKay, G., 1999. Pseudo-second order model for sorption processes. Process Biochem. 34, 451–465. https://doi.org/10.1016/S0032-9592(98)00112-5.

Hu, X.C., Andrews, D.Q., Lindstrom, A.B., Bruton, T.A., Schaider, L.A., Grandjean, P., Lohmann, R., Carignan, C.C., Blum, A., Balan, S.A., 2016. Detection of poly-and perfluoroalkyl substances (PFASs) in US drinking water linked to industrial sites, military fire training areas, and wastewater treatment plants. Environ. Sci. Technol. Lett. 3, 344–350. https://doi.org/10.1021/acs.estlett.6b00260.

Hu, Z., Song, X., Wei, C., Liu, J., 2017. Behavior and mechanisms for sorptive removal of perfluorooctane sulfonate by layered double hydroxides. Chemosphere 187, 196–205. https://doi.org/10.1016/j.chemosphere.2017.08.082.

Ishikawa, T., Matsumoto, K., Kandori, K., Nakayama, T., 2007. Anion-exchange and thermal change of layered zinc hydroxides formed in the presence of Al(III). Colloids Surf. A Physicochem. Eng. Asp. 293, 135–145. https://doi.org/10.1016/j.colsurfa.2006.07.018.

Ji, B., Kang, P., Wei, T., Zhao, Y., 2020. Challenges of aqueous per-and polyfluoroalkyl substances (PFASs) and their foreseeable removal strategies. Chemosphere 250, 126316. https://doi.org/10.1016/j.chemosphere.2020.126316.

Johnson, R.L., Anschutz, A.J., Smolen, J.M., Simcik, M.F., Penn, R.L., 2007. The adsorption of perfluorooctane sulfonate onto sand, clay, and iron oxide surfaces. J. Chem. Eng. Data 52, 1165–1170. https://doi.org/10.1021/je060285g.

Kotthoff, M., Müller, J., Jürling, H., Schlummer, M., Fiedler, D., 2015. Perfluoroalkyl and polyfluoroalkyl substances in consumer products. Environ. Sci. Pollut. Res. 22, 14546–14559. https://doi.org/10.1007/s11356-015-4202-7.

Kunacheva, C., Fujii, S., Tanaka, S., Seneviratne, S., Lien, N.P.H., Nozoe, M., Kimura, K., Shivakoti, B.R., Harada, H., 2012. Worldwide surveys of perfluorooctane sulfonate (PFOS) and perfluorooctanoic acid (PFOA) in water environment in recent years. Water Sci. Technol. 66, 2764–2771. https://doi.org/10.2166/wst.2012.518.

Li, C., Schäffer, A., Séquaris, J.-M., László, K., Tóth, A., Tombácz, E., Vereecken, H., Ji, R., Klumpp, E., 2012. Surface-associated metal catalyst enhances the sorption of perfluorooctanoic acid to multi-walled carbon nanotubes. J. Colloid Interface Sci. 377, 342–346. https://doi.org/10.1016/j.jcis.2012.03.038.

Li, F., Duan, J., Tian, S., Ji, H., Zhu, Y., Wei, Z., Zhao, D., 2020. Short-chain per-and polyfluoroalkyl substances in aquatic systems: occurrence, impacts and treatment. Chem. Eng. J. 380, 122506. https://doi.org/10.1016/j.cej.2019.122506.

Matilainen, A., Gjessing, E.T., Lahtinen, T., Hed, L., Bhatnagar, A., Sillanpää, M., 2011. An overview of the methods used in the characterisation of natural organic matter (NOM) in relation to drinking water treatment. Chemosphere 83, 1431–1442. https://doi.org/10.1016/j.chemosphere.2011.01.018.

Merino, N., Qu, Y., Deeb, R.A., Hawley, E.L., Hoffmann, M.R., Mahendra, S., 2016. Degradation and removal methods for perfluoroalkyl and polyfluoroalkyl substances in water. Environ. Eng. Sci. 33, 615–649. https://doi.org/10.1089/ees.2016.0233.

Min, X., Trujillo, D., Huo, J., Dong, Q., Wang, Y., 2020. Amine-bridged periodic mesoporous organosilica nanomaterial for efficient removal of selenate. Chem. Eng. J. 396, 125278. https://doi.org/10.1016/j.cej.2020.125278.

Mishra, G., Dash, B., Pandey, S., 2018. Layered double hydroxides: a brief review from fundamentals to application as evolving biomaterials. Appl. Clay Sci. 153, 172–186. https://doi.org/10.1016/j.clay.2017.12.021.

Olfs, H.W., Torres-Dorante, L., Eckelt, R., Kosslick, H., 2009. Comparison of different synthesis routes for Mg–Al layered double hydroxides (LDH): characterization of the structural phases and anion exchange properties. Appl. Clay Sci. 43, 459–464. https://doi.org/10.1016/j.clay.2008.10.009.

Park, M., Daniels, K.D., Wu, S., Ziska, A.D., Snyder, S.A., 2020a. Magnetic ion-exchange (MIEX) resin for perfluorinated alkylsubstance (PFAS) removal in groundwater: roles of atomic charges for adsorption. Water Res. 181, 115897. https://doi.org/10.1016/j.watres.2020.115897.

Park, M., Wu, S., Lopez, I.J., Chang, J.Y., Karanfil, T., Snyder, S.A., 2020b. Adsorption of perfluoroalkyl substances (PFAS) in groundwater by granular activated carbons: roles of hydrophobicity of PFAS and carbon characteristics. Water Res. 170, 115364. https://doi.org/10.1016/j.watres.2019.115364.

Post, G.B., Louis, J.B., Cooper, K.R., Boros-Russo, B.J., Lippincott, R.L., 2009. Occurrence and potential significance of perfluorooctanoic acid (PFOA) detected in New Jersey public drinking water systems. Environ. Sci. Technol. 43, 4547–4554. https://doi.org/10.1021/es900301s.

Schultz, M.M., Barofsky, D.F., Field, J.A., 2004. Quantitative determination of fluorotelomer sulfonates in groundwater by LC MS/MS. Environ. Sci. Technol. 38, 1828–1835. https://doi.org/10.1021/es035031j.

Seftel, E.M., Popovici, E., Mertens, M., Witte, K.D., Tendeloo, G.V., Cool, P., Vansant, E. F., 2008. Zn–Al layered double hydroxides: synthesis, characterization and photocatalytic application. Microporous Mesoporous Mater. 113, 296–304. https://doi.org/10.1016/j.micromeso.2007.11.029.

Seida, Y., Nakano, Y., 2002. Removal of phosphate by layered double hydroxides containing iron. Water Res. 36, 1306–1312. https://doi.org/10.1016/S0043-1354(01)00340-2.

Sharifan, H., Bagheri, M., Wang, D., Burken, J.G., Higgins, C.P., Liang, Y., Liu, J., Schaefer, C.E., Blotevogel, J., 2021. Fate and transport of per-and polyfluoroalkyl substances (PFASs) in the vadose zone. Sci. Total Environ. 145427 https://doi.org/10.1016/j.scitotenv.2021.145427.

Sun, X., Imai, T., Sekine, M., Higuchi, T., Yamamoto, K., Kanno, A., Nakazono, S., 2014. Adsorption of phosphate using calcined Mg3–Fe layered double hydroxides in a fixed-bed column study. J. Ind. Eng. Chem. 20, 3623–3630. https://doi.org/10.1016/j.jiec.2013.12.057.

Theiss, F.L., Ayoko, G.A., Frost, R.L., 2013. Thermogravimetric analysis of selected layered double hydroxides. J. Therm. Anal. Calorim. 112, 649–657. https://doi.org/10.1007/s10973-012-2584-z.

Vu, C.T., Wu, T., 2020. Adsorption of short-chain perfluoroalkyl acids (PFAAs) from water/wastewater. Environ. Sci. Water Res. Technol. 6, 2958–2972. https://doi.org/10.1039/D0EW00468E.

Wang, M., Orr, A.A., Jakubowski, J.M., Bird, K.E., Casey, C.M., Hearon, S.E., Tamamis, P., Phillips, T.D., 2021. Enhanced adsorption of per-and polyfluoroalkyl substances (PFAS) by edible, nutrient-amended montmorillonite clays. Water Res. 188, 116534. https://doi.org/10.1016/j.watres.2020.116534.

Wang, Q., O'Hare, D., 2012. Recent advances in the synthesis and application of layered double hydroxide (LDH) nanosheets. Chem. Rev. 112, 4124–4155. https://doi.org/10.1021/cr200434v.

Wang, Z., Cousins, I.T., Scheringer, M., Hungerbuehler, K., 2015. Hazard assessment of fluorinated alternatives to long-chain perfluoroalkyl acids (PFAAs) and their precursors: status quo, ongoing challenges and possible solutions. Environ. Int. 75, 172–179. https://doi.org/10.1016/j.envint.2014.11.013.

Wang, Z., Cousins, I.T., Scheringer, M., Hungerbühler, K., 2013. Fluorinated alternatives to long-chain perfluoroalkyl carboxylic acids (PFCAs), perfluoroalkane sulfonic acids (PFSAs) and their potential precursors. Environ. Int. 60, 242–248. https://doi.org/10.1016/j.envint.2013.08.021.

Wang, Z., DeWitt, J.C., Higgins, C.P., Cousins, I.T., 2017. A never-ending story of per-and polyfluoroalkyl substances (PFASs)? Environ. Sci. Technol. 51, 2508–2518. https://doi.org/10.1021/acs.est.6b04806.

Wanninayake, D.M., 2021. Comparison of currently available PFAS remediation technologies in water: a review. J. Environ. Manag. 283, 111977. https://doi.org/10.1016/j.jenvman.2021.111977.

Xiao, F., Hanson, R.A., Golovko, S.A., Golovko, M.Y., Arnold, W.A., 2018. PFOA and PFOS are generated from zwitterionic and cationic precursor compounds during water disinfection with chlorine or ozone. Environ. Sci. Technol. Lett. 5, 382–388. https://doi.org/10.1021/acs.estlett.8b00266.

Xiao, F., Zhang, X., Penn, L., Gulliver, J.S., Simcik, M.F., 2011. Effects of monovalent cations on the competitive adsorption of perfluoroalkyl acids by kaolinite: experimental studies and modeling. Environ. Sci. Technol. 45, 10028–10035. https://doi.org/10.1021/es202524y.

Xiao, L., Ling, Y., Alsbaiee, A., Li, C., Helbling, D.E., Dichtel, W.R., 2017. β-Cyclodextrin polymer network sequesters perfluorooctanoic acid at environmentally relevant concentrations. J. Am. Chem. Soc. 139, 7689–7692. https://doi.org/10.1021/jacs.7b02381.

Yang, H., Wang, Y., Bender, J., Xu, S., 2019. Removal of arsenate and chromate by lanthanum-modified granular ceramic material: the critical role of coating temperature. Sci. Rep. 9, 1–12. https://doi.org/10.1038/s41598-019-44165-8.

Yang, K., Yan, L.-g., Yang, Y.-m., Yu, S.-j., Shan, R.-r., Yu, H.-q., Zhu, B.-c., Du, B., 2014. Adsorptive removal of phosphate by Mg–Al and Zn–Al layered double hydroxides: kinetics, isotherms and mechanisms. Separ. Purif. Technol. 124, 36–42. https://doi.org/10.1016/j.seppur.2013.12.042.

Yang, Y., Yang, M., Zheng, Z., Zhang, X., 2020a. Highly effective adsorption removal of perfluorooctanoic acid (PFOA) from aqueous solution using calcined layer-like Mg-Al hydrotalcites nanosheets. Environ. Sci. Pollut. Res. 27, 13396–13408. https://doi.org/10.1007/s11356-020-07892-4.

Yang, Y., Zheng, Z., Ji, W., Xu, J., Zhang, X., 2020b. Insights to perfluorooctanoic acid adsorption micro-mechanism over Fe-based metal organic frameworks: combining computational calculation with response surface methodology. J. Hazard Mater. 395, 122686. https://doi.org/10.1016/j.jhazmat.2020.122686.

You, Y., Vance, G.F., Zhao, H., 2001. Selenium adsorption on Mg–Al and Zn–Al layered double hydroxides. Appl. Clay Sci. 20, 13–25. https://doi.org/10.1016/S0169-1317(00)00043-0.

Yu, J., Lv, L., Lan, P., Zhang, S., Pan, B., Zhang, W., 2012. Effect of effluent organic matter on the adsorption of perfluorinated compounds onto activated carbon. J. Hazard Mater. 225, 99–106. https://doi.org/10.1016/j.jhazmat.2012.04.073.

Yu, Q., Zhang, R., Deng, S., Huang, J., Yu, G., 2009. Sorption of perfluorooctane sulfonate and perfluorooctanoate on activated carbons and resin: kinetic and isotherm study. Water Res. 43, 1150–1158. https://doi.org/10.1016/j.watres.2008.12.001.

Zhang, B., Dong, Z., Sun, D., Wu, T., Li, Y., 2017. Enhanced adsorption capacity of dyes by surfactant-modified layered double hydroxides from aqueous solution. J. Ind. Eng. Chem. 49, 208–218. https://doi.org/10.1016/j.jiec.2017.01.029.

Zhang, D., Luo, Q., Gao, B., Chiang, S.-Y.D., Woodward, D., Huang, Q., 2016. Sorption of perfluorooctanoic acid, perfluorooctane sulfonate and perfluoroheptanoic acid on granular activated carbon. Chemosphere 144, 2336–2342. https://doi.org/10.1016/j.chemosphere.2015.10.124.

Zhang, D., Zhang, W., Liang, Y., 2019. Adsorption of perfluoroalkyl and polyfluoroalkyl substances (PFASs) from aqueous solution-A review. Sci. Total Environ. 694, 133606. https://doi.org/10.1016/j.scitotenv.2019.133606.

Zhang, T., Li, Q., Xiao, H., Lu, H., Zhou, Y., 2012. Synthesis of Li–Al layered double hydroxides (LDHs) for efficient fluoride removal. Ind. Eng. Chem. Res. 51, 11490–11498. https://doi.org/10.1021/ie300863x.